MATERIALS ENGINEERING

10.1126/sciadv.1501779

Programmable colloidal molecules from sequential capillarity-assisted particle assembly

Songbo Ni,[1,2] Jessica Leemann,[1,2] Ivo Buttinoni,[1] Lucio Isa,[1]* Heiko Wolf[2]*

The assembly of artificial nanostructured and microstructured materials which display structures and functionalities that mimic nature's complexity requires building blocks with specific and directional interactions, analogous to those displayed at the molecular level. Despite remarkable progress in synthesizing "patchy" particles encoding anisotropic interactions, most current methods are restricted to integrating up to two compositional patches on a single "molecule" and to objects with simple shapes. Currently, decoupling functionality and shape to achieve full compositional and geometrical programmability remains an elusive task. We use sequential capillarity-assisted particle assembly which uniquely fulfills the demands described above. This is a new method based on simple, yet essential, adaptations to the well-known capillary assembly of particles over topographical templates. Tuning the depth of the assembly sites (traps) and the surface tension of moving droplets of colloidal suspensions enables controlled stepwise filling of traps to "synthesize" colloidal molecules. After deposition and mechanical linkage, the colloidal molecules can be dispersed in a solvent. The template's shape solely controls the molecule's geometry, whereas the filling sequence independently determines its composition. No specific surface chemistry is required, and multifunctional molecules with organic and inorganic moieties can be fabricated. We demonstrate the "synthesis" of a library of structures, ranging from dumbbells and triangles to units resembling bar codes, block copolymers, surfactants, and three-dimensional chiral objects. The full programmability of our approach opens up new directions not only for assembling and studying complex materials with single-particle-level control but also for fabricating new microscale devices for sensing, patterning, and delivery applications.

INTRODUCTION

Colloidal particles have long been used as model systems to investigate the fundamental properties of materials (*1*) and as building blocks for spontaneous and directed assembly (*2*–*4*). The quest to mimic nature's complexity in the range of achievable structures beyond isotropic systems requires colloids with directional and specific interactions (*5*, *6*) and has prompted tremendous efforts in particle synthesis and fabrication (*7*–*9*). In the (sub)micrometer range, the most successful systems to date are patchy particles (that is, colloids with heterogeneous surface regions in predetermined positions), which have successfully been used to assemble structures resembling simple molecules (*10*, *11*), responsive filaments (*12*), and complex lattices (*13*). However, most current fabrication strategies for patchy colloids (*8*, *14*, *15*) suffer from a significant limitation—particle geometry, composition, and functionality cannot be controlled independently at will. Ultimately, highly complex superstructures require more information encoded in their colloidal building blocks.

Here, we demonstrate a new bottom-up method termed "sequential capillarity-assisted particle assembly" (sCAPA) that uniquely overcomes these limitations. Traditional capillarity-assisted particle assembly (CAPA) works by moving the meniscus of an aqueous colloidal suspension droplet over a topographical template, whereby capillary forces at the meniscus place the particles into designated positions (*16*–*18*). The method is most commonly used as a patterning tool, in which complex templates with specific structures are used to assemble and, optionally, transfer (by printing) particle patterns for applications in nanoelectronics (*19*, *20*), sensing (*21*), plasmonics (*22*, *23*), and nanopatterning (*17*, *24*). Here, we turn the method into a novel and flexible tool for the synthesis of fully programmable and multifunctional colloidal clusters ("colloidal molecules") by exploiting a series of simple, yet essential, adaptations to the state of the art.

In CAPA, the geometry of the traps (both depth and lateral shape and size) typically closely matches the geometry of the target structures to ensure complete filling with high efficiency. Tuning the number of different kinds of particles assembled in a single trap is a more complicated task—only achieved, until recently, in successive steps using smaller (*16*) or differently shaped (*23*) particles to fill interstices. Encoding the composition by such methods is typically limited to binary systems, either due to constraints in the fabrication of complex-shaped templates to place many levels of differently sized and shaped particles in specific positions or due to the formation of unspecific multiple layers when using smaller particles over prefilled assembly sites.

We recently found that, in addition to manipulating its lateral size and shape, tuning the trap depth and the surface tension of the aqueous droplet enables robust control of the number of particles assembled in single deposition steps (*25*). Consequently, there is a new, accurate route to reprogramming the composition of the structures deposited in a single trap by refilling it with different particles.

The control of the number of assembled particles in each deposition is the result of the interplay between the trap geometry and the forces acting on the particles in the trap. As schematically shown in Fig. 1A, the front particle (particle 1) interacts first with the moving meniscus and then experiences a downward capillary force F_c perpendicular to the meniscus. This force is partly transmitted to the rear particle (particle 2) and can lead to an upward force F'_c in the presence of small vertical displacements, which can push particle 2 out of the trap during

[1]Laboratory for Interfaces, Soft Matter, and Assembly, Department of Materials, ETH Zurich, Vladimir-Prelog-Weg 5, 8093 Zurich, Switzerland. [2]IBM Research–Zurich, Säumerstrasse 4, 8803 Rüschlikon, Switzerland.
*Corresponding author. E-mail: lucio.isa@mat.ethz.ch (L.I.); hwo@zurich.ibm.com (H.W.)

further retraction of the meniscus. The effect of the upward force F'_c can be conveniently increased by reducing the trap depth (or vice versa, reduced using deeper traps) for a given surface tension. More details on a mechanical model describing this process can be found in the study by Ni *et al.* (*25*). Consequently, we can selectively assemble single particles when the trap is shallow ($d \approx r$, where d is trap depth and r is particle radius), whereas the trap is completely filled for larger depths ($d \approx 2r$). A crucial finding, which defines the core principle of sCAPA, is that only a single particle is assembled in each deposition step, even in complex traps, as illustrated for the first step of the filling of long traps as well as for triangular traps in Fig. 1 (B and C, respectively). Drying causes strong adhesion to the template such that already assembled particles do not leave the traps and the remaining space can be filled with new particles one at a time, in which case the last preassembled particle defines a new trap geometry. This new concept enables complete encoding of the composition beyond binary systems and does not require any specific surface chemistry of the assembled particles. Here, we demonstrate the potential of sCAPA as a synthesis method by fabricating hybrid colloidal molecules ranging from dumbbells and triangles to particles resembling bar codes, block copolymers, surfactants, and three-dimensional (3D) chiral objects, with precise compositional and material programmability in each step. The geometry of the template defines the molecule shape independently of its composition, which is controlled by choosing the particle(s) to be deposited in each step. After deposition, the clusters are mechanically linked, harvested, and dispersed in solution.

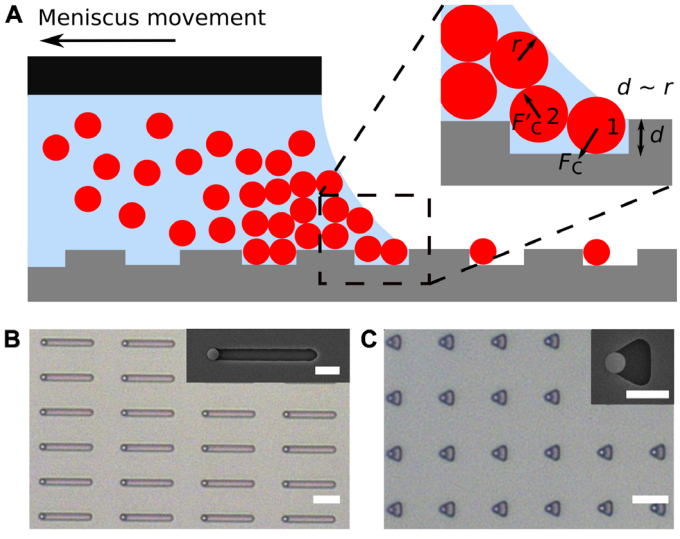

Fig. 1. Working principle of depositing a single particle in a large trap. (**A**) Scheme of the assembly in rectangular traps ($1.2 \times 2.2\ \mu m^2$), with the trap depth d approximately equal to the particle radius r ($d = 510$ nm, $r = 500$ nm). The zoom shows the front particle (particle 1) experiencing a downward capillary force F_c perpendicular to the meniscus. The force F_c partly transmits to the rear particle (particle 2), leading to an upward force F'_c in the presence of a small vertical displacement, which pushes particle 2 out of the trap. Eventually, only particle 1 is assembled in the trap. (**B** and **C**) Trapping only a single particle is also found in 10-μm-long traps (B) and in triangular traps (C). The insets to (B) and (C) are the corresponding scanning electron microscopy (SEM) images. Scale bars, 5 μm (B and C) and 2 μm (insets to B and C).

RESULTS

Here, sCAPA is applied to the preparation of a variety of complex-shaped, multifunctional colloidal molecules. Unless otherwise specified, the following experimental parameters are used in all depositions. The spherical particles used are 1.0 μm in diameter, and the depth of all traps, fabricated in silicone elastomer [poly(dimethylsiloxane) (PDMS)] templates, is optimized to be approximately equivalent to the particle radius (510 ± 10 nm) (*25*). A surfactant mixture (0.1 mM SDS + 0.01 wt % Triton X-45), providing a water-air surface tension of ~29 mN m^{-1}, is used (for more details, see Materials and Methods).

We first use sCAPA to assemble programmable linear clusters by sequentially depositing different particles one by one in line-shaped traps, as schematically shown in Fig. 2A. Lines of different dimensions were used, with a fixed width close to the particle diameter and varying lengths on the order of several particle diameters (see Materials and Methods). The meniscus was positioned perpendicular to the long axis of the traps and moved in the direction of their long axis.

Figure 2 (B and C) shows green-red-blue (G-R-B) and blue-green-red-blue (B-G-R-B) bar-code–like colloidal chains, in which we sequentially assembled different fluorescent polystyrene (PS) particles three and four times, respectively (SEM images are reproduced in fig. S1, A and B). The yield for both depositions reaches 83% over an area of several tens of square millimeters. The numbers of particle clusters

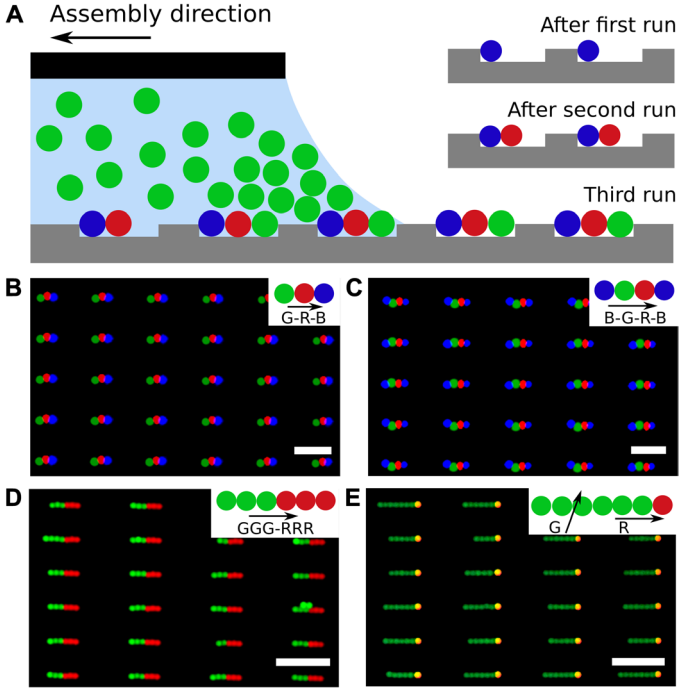

Fig. 2. One-dimensional linear colloidal chains assembled by sCAPA. (**A**) Scheme illustrating the stepwise sequence for fabricating multicomponent colloidal chains. (**B** to **E**) One-dimensional linear PS colloidal chains assembled using different particles and sequences, resembling bar-code chains (B and C), block copolymers (D), and surfactants (E) (merged fluorescence images). The insets show the specific assembly sequence and directions in each case. Note that in the assembly of surfactant-like colloidal chains, the assembly direction was rotated by ~80° for the second step (inset to E). Scale bars, 5 μm (B and C) and 10 μm (D and E).

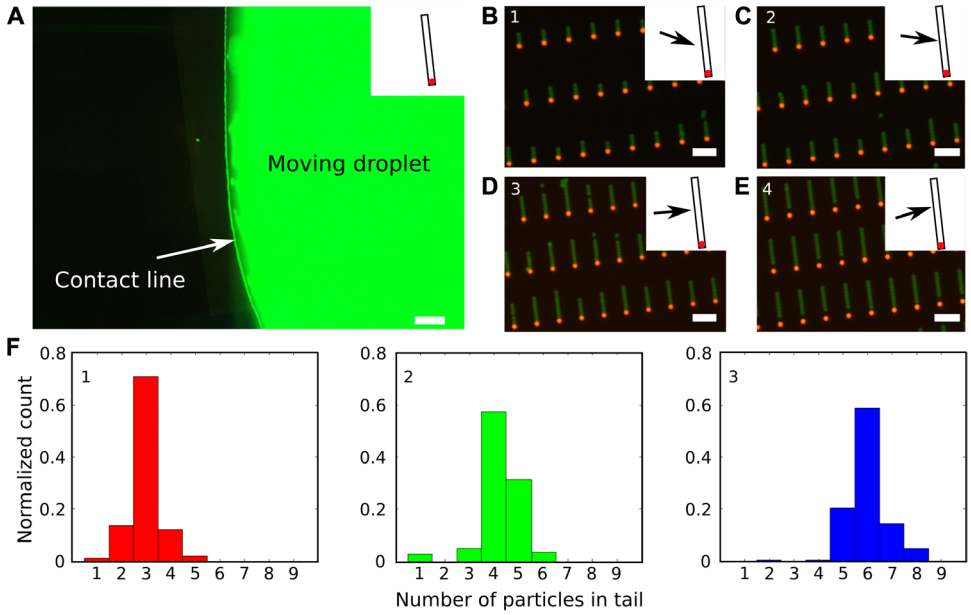

Fig. 3. Polydispersity in the tail length of surfactant-like colloidal chains. (**A**) Fluorescence image of the second assembly step for the formation of surfactant-like chains, demonstrating the variability of the local assembly direction caused by the curvature of the moving droplet. The inset shows the orientation of the traps. Scale bar, 200 μm. (**B** to **E**) Merged fluorescence images taken at different positions along the contact line. The arrows in the insets schematically represent the local assembly direction relative to the traps. Scale bars, 5 μm. (**F**) Histograms of the distribution of tail lengths, that is, the number of particles in the tail corresponding to cases 1, 2, and 3 shown in (B) to (D). For each histogram, 140 colloidal molecules were analyzed. (E) There is no tail-length count for position 4 because, in that case, most tails are pushed to the opposite end of the trap, leaving a gap between the "head" and the "tail" particles.

and the throughput can be scaled up by increasing the size of the template or by using parallel depositions (*26*), as discussed later. The number of possible sequences (M^N, where M is the number of available particle types and N is the trap length/particle diameter) increases significantly with trap length. Figure 2D shows GGG-RRR (G, green; R, red) chains whose composition is precisely encoded in each of the six assembly steps, creating an architecture analogous to that of block copolymers.

Selectivity in the number of trapped colloids also enables precise control of the composition by tuning the orientation of the moving meniscus relative to the trap direction. We fabricated surfactant-like colloidal chains (Fig. 2E) with a single head particle followed by a tail composed of different PS particles (SEM image in fig. S1C). The first deposition step, which selectively placed a single head particle in each trap, was performed with the meniscus moving in the direction of the trap long axis, as described above (see movie S1). Then, the second assembly step was performed after turning the template by ~80° relative to the first one so that all the particles forming the long tails could be deposited at once (movie S2 and inset to Fig. 3A). The second assembly step led to a certain degree of polydispersity in the tail length or even to the absence of contact between the head and the tail (Fig. 3), caused by the varying local assembly direction along the curved contact line of the meniscus (Fig. 3A). Although this curvature has only little influence on the bar code and block copolymer colloidal chains assembled one by one, it does affect the simultaneous assembly of multiple particles in the tails. The tail is longer when the contact line is more parallel to the long axis, whereas steeper angles lead to shorter chains (Fig. 3, B to D and F). In the extreme case where the droplet contact line forms a negative angle with the long axis of the trap, the tail particles are pushed into the opposite end of the trap, away from the previously assembled head particle. In this case, the tail and the head remain separated (Fig. 3E), and the particles cannot be linked and harvested. These issues can be overcome by appropriately engineering the shape of the meniscus and the orientation of the traps. A straight contact line over the entire template is the ideal solution, which could be achieved, for instance, by using a microfluidic chip to confine the moving droplet and continuously supply the suspension to the assembly front (*27*). The assembly of colloidal surfactants demonstrates nonetheless that changing the orientation of the traps enables additional control of the deposition of complex structures, which is crucial to the next step described below.

sCAPA can also be applied on traps that are not line-shaped for assembling clusters with different planar geometries. Using templates with triangle-shaped traps, we carried out three consecutive assembly steps to place three different particles in each corner of the traps, as schematically illustrated in Fig. 4A. The arrows in Fig. 4A represent the local assembly direction (that is, the direction in which the meniscus moves). The size of the trap influences both the yield and the structure of the assembled trimers. The yield of the trimers was between 82 and 89% once the traps were large enough to accommodate three particles (see Fig. 4, B and C, and fig. S2). Trimers can either be close-packed (Fig. 4D) or separated (Fig. 4E) by increasing the size of the trap. Moreover, the separated trimers offer the possibility to go beyond planar cluster geometries and to prepare 3D colloidal clusters by placing a fourth, smaller particle on top. Figure 4F shows such an assembly strategy, in which three already assembled particles defined

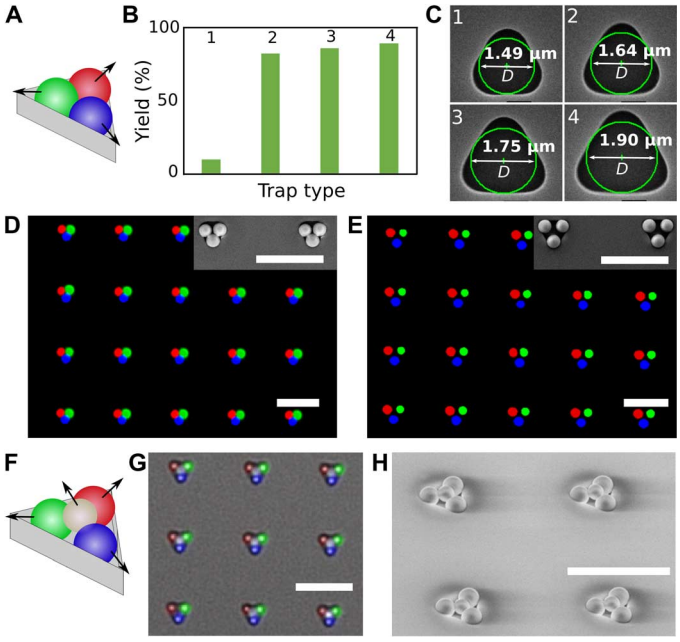

Fig. 4. Two-dimensional and 3D PS colloidal molecules assembled by sCAPA. (**A**) Scheme showing local sequential assembly directions. (**B** and **C**) Yield of colloidal trimers with three different lobes (B) in traps of different sizes (C). The numbers on top of the columns in (B) correspond to the numbers assigned to the traps in (C). *D* indicates the diameter of the circle inscribed to the triangular trap. (**D** and **E**) Merged fluorescence images of close-packed (D) and separated (E) colloidal trimers with three different lobes. Insets depict the corresponding SEM micrographs. (**F** to **H**) Three-dimensional chiral clusters with four different lobes. (F) Scheme of assembly steps and directions. (G) Overlay of fluorescence and bright-field images. (H) SEM micrograph with a 45° incident angle. Scale bars, 5 μm.

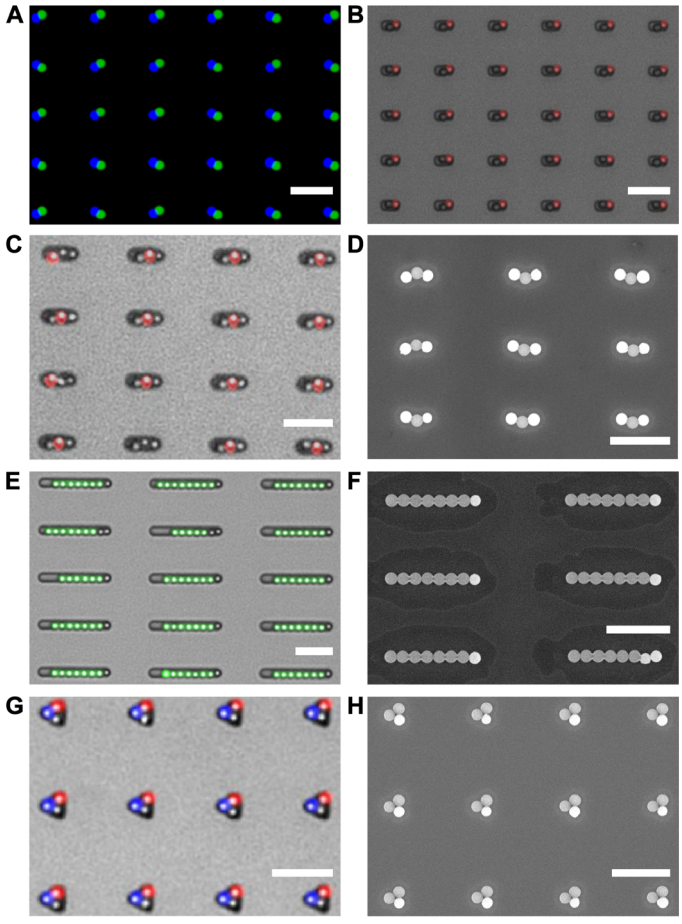

Fig. 5. Multimaterial linear and nonlinear clusters. (**A** and **B**) Asymmetric dumbbells assembled from carboxylate PS/amine PS (merged fluorescence image) (A) and from PS and SiO_2 (overlay of fluorescence and bright-field image) (B). (**C** and **D**) Three-particle colloidal chains with a magnetic SiO_2 particle (left), a PS particle (middle), and a nonfunctionalized SiO_2 particle (right) [energy-dispersive x-ray (EDX) spectroscopy; see fig. S4]. Overlay of a fluorescence image with a bright-field image on the template (C) and SEM image after the printing of the particles onto a silicon substrate (D). (**E** and **F**) Surfactant-like colloidal chains with a magnetic SiO_2 particle followed by a tail of PS particles. Overlay of a fluorescence image with a bright-field image on the template (E) and SEM image after the printing of the particles onto a silicon substrate (F). (**G** and **H**) Trimers with a magnetic particle and two different PS particles. Overlay of a fluorescence image with a bright-field image on the template (G) and SEM image after the printing of the particles onto a silicon substrate (H). Scale bars, 5 μm.

a new trapping site for the fourth one. Figure 4G shows the overlay of fluorescence and bright-field images, in which the bright spots in the center of the triangles indicate the presence of a fourth particle with a 0.78-μm diameter. Figure 4H shows the corresponding SEM image with a 45° incident angle, illustrating that the fourth particle sits in the middle of the cluster and off the plane of the previously assembled particles. Furthermore, by controlling the deposition sequence, 3D clusters with either clockwise or counterclockwise chiral symmetry can be constructed.

An additional strength of the presented technique is that it does not rely on any specific chemistry or material properties, which makes it possible to assemble a wide variety of materials. We sequentially assembled amine- and carboxylate-functionalized PS particles and silica particles, with or without magnetic properties, into different combinations using line and triangle traps, as shown in Fig. 5 (A to H). Chemically asymmetric dumbbells (Fig. 5, A and B) can be assembled with an approximate yield of 95% over a pattern area of 5 × 12 mm^2, corresponding to ~1.5 million dumbbells (see the example of amine PS/carboxylate PS dumbbells in fig. S3). Moreover, we prepared longer multifunctional chains (Fig. 5, C and D, and fig. S4), colloidal surfactants with a magnetic particle as head and PS particles in the tail (Fig. 5, E and F), and trimers with a magnetic particle and two different fluorescent PS particles (Fig. 5, G and H).

For further applications, the assembled colloidal clusters need to be released from the template after sCAPA. Figure 6 schematically shows the harvesting process. After assembly, the clusters are first linked mechanically via a sintering step at a temperature below the glass transition temperature (T_g) of bulk PS, which melts the particles together at the surface where they are in contact, without entirely deforming them (see Fig. 6 and fig. S5). In the multimaterial clusters, the PS particles act as an adhesive linking the inorganic particles. Finally, for the harvesting of the linked clusters from the template, we developed a place-and-pick method

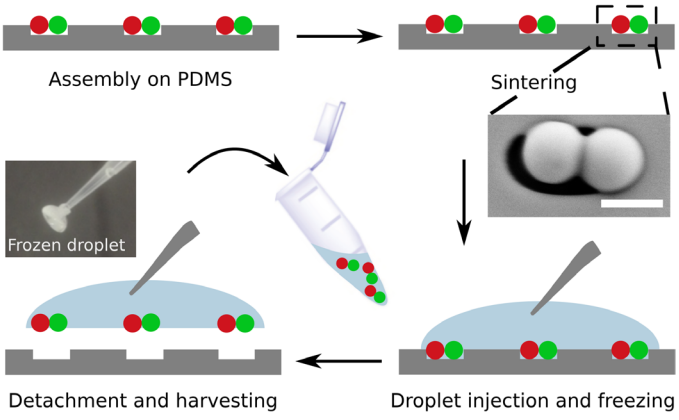

Fig. 6. Scheme of the harvesting process. The SEM image shows a linked PS-PS dumbbell in a trap on the template. Scale bar, 1 μm. The micrograph shows the frozen water droplet attached to a micropipette tip.

that features a targeted, chemical-free, and high-yield transfer (see Fig. 6 and fig. S6). The process works by placing and freezing a small water droplet (20 μl) on the area of interest; the frozen droplet is subsequently picked up from the surface and stored. In this process, the clusters are embedded in ice upon freezing of the water droplet, resulting in strong adhesion and possibly mechanical interlocking, which enables detachment from the template.

Figure 7 (A to C) shows harvested and dried R-G PS dumbbells and R-G-B PS bar-code chains and trimers, respectively. Figure 7D shows snapshots of colloidal surfactants with PS tails that are one particle (left), three particles (middle), and seven particles (right) long and have a magnetic silica head that are dispersed in water and undergoing Brownian motion (movies S3 to S5). The magnetic head allows the actuation of the clusters with external fields, in either rotation, oscillation, or translation mode (movies S6 to S8), offering new possibilities of manipulating these multicomponent colloids for directed assembly (*28*) or delivery applications (*29*, *30*).

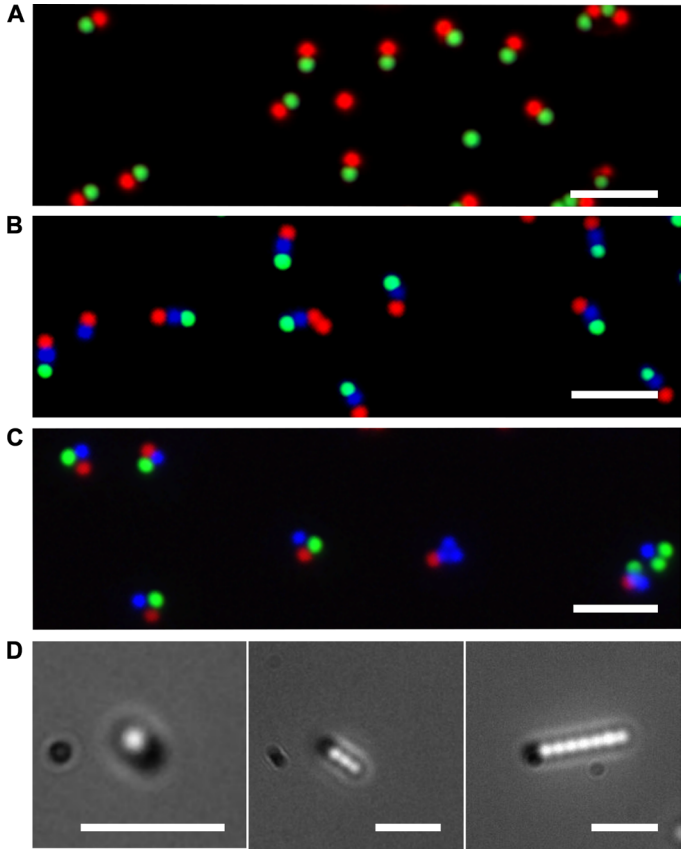

Fig. 7. Harvested clusters. (**A** to **C**) Merged fluorescence images of harvested and dried R-G PS dumbbells (A), R-B-G PS three-particle chains (B), and R-G-B PS three-particle trimers (C) on silicon substrates. (**D**) Snapshots of colloidal surfactants with PS tails that are one particle (left), three particles (middle), and seven particles (right) long and have a magnetic head. The clusters are in solution and undergo Brownian motion. The images were captured by combining the fluorescence and transmission channels. Scale bars, 5 μm.

DISCUSSION

In conclusion, we presented a simple concept to fabricate a large range of multifunctional and programmable colloidal molecules by means of sequential capillary assembly over topographical templates. Tuning the trap geometry, and especially its depth around the particle radius for a given surface tension of the suspension, enables the selective stepwise filling of the traps with any predefined sequence. Changing the orientation of the droplet motion relative to the trap makes it also possible to fabricate 1D, 2D, and 3D colloidal molecules.

The method lends itself to producing sufficient amounts of colloidal molecules to not only to perform single-molecule studies but also to look at the assembly and collective effects of such colloidal molecules. As previously mentioned for difunctional dumbbells, in a typical experiment, we can assemble on the order of 1×10^6 colloidal molecules on a template area of 5×12 mm^2. In the case of dumbbells, this corresponds to a densely packed monolayer of approximately 2 mm^2 (assuming that the dumbbells are lying flat), amply sufficient, for instance, for studies of particle monolayers at fluid interfaces or the collective behavior of particle assemblies confined by external fields (*31*).

Typical time scales for sCAPA are on the order of 100 min per deposition step, using a deposition speed of 2 μm s^{-1}. The sintering and harvesting steps only take a few minutes and are not rate-limiting. For higher throughput, the template area can be easily enlarged, the assembly speed can be increased (5 to 20 μm s^{-1}, depending on the type of particle), and microfluidic devices (*26*, *27*) can be used to parallelize the assembly process. With these optimizations, we envisage that batches of up to 1×10^8 molecules could be produced within similar times. The building blocks demonstrated in this report constitute only the surface of a library of programmable and multifunctional colloidal clusters that may attract interest in a range of fundamental and applied fields, as discussed below.

The capability of encoding particle sequences in 1D linear colloidal chains enables the fabrication of a variety of anisotropic particles acting as building blocks for responsive assembly (*32*, *33*), which has the potential for object recognition through lock-and-key of complementary sequences. It may be used to create bar-code particles for multiplex assays (*34*, *35*). Surfactant-like chains with tunable heads and tails can be used as models to shed light on the assembly of molecular

surfactants at the single-molecule level or to help answer open questions regarding the wetting, orientation, and dynamics of asymmetric colloids at fluid interfaces (*36*, *37*). Two-dimensional triangular clusters with three differently labeled lobes could be used as precise tracers for 3D particle tracking to extract the full rotational and translational dynamics in complex environments (*38*). Multifunctional 3D tetramers may finally be used to direct the assembly of complex lattices for optical materials (*39*, *40*). In addition, the new options provided by sCAPA are likely to attract interest from the numerical simulations community because, with sCAPA, one can now realize real particles that are close to idealized models and whose design can be directed to obtain target structures. Other interesting new directions could be the inclusion of soft particles as linkers, to produce molecules with internal degrees of freedom, and extension to the deposition of hydrophobic particles from organic solvents, to further broaden the range of moieties in colloidal molecules produced by sCAPA. Given the flexibility in the design of trap geometries and the fast progress in particle synthesis, more complex colloidal molecules are expected in the future, which will be a powerful tool not only for assembling complex materials and studying their properties at the single-molecule level but also for fabricating new microscale devices for sensing (*41*), patterning (*42*), and delivery applications (*29*).

MATERIALS AND METHODS

Colloidal suspensions

Fluorescent PS particles with a diameter of 1 μm (red, R0100; green, G0100; blue, B0100; polydispersity < 5%), nonfluorescent PS particles with a diameter of 0.78 μm (W080C-002; polydispersity < 5%), and plain silica particles with a diameter of 1 μm (8100; polydispersity < 5%) were purchased from Thermo Scientific. Magnetic particles (iron oxide nanoparticles in a silica matrix) with a diameter of 0.96 ± 0.05 μm (SiO_2-MAG-AR359) were purchased from microParticles GmbH. All particles were suspended in an aqueous mixture of 0.1 mM SDS and 0.01 wt % Triton X-45 (corresponding to a water-air surface tension of 29 mN m^{-1}), except for the particles with a diameter of 0.78 μm, which were prepared in a mixture of 0.25 mM SDS and 0.025 wt % Triton X-45 (corresponding to a water-air surface tension of approximately 27 mN m^{-1}).

Template fabrication

The PDMS templates were fabricated according to the method introduced by Geissler *et al.* (*43*). The depth of the trap was 510 ± 10 nm. The linear traps had a width of 1.2 ± 0.2 μm and lengths of 2.1 ± 0.1, 3.1 ± 0.1, 4.1 ± 0.1, and 10.0 ± 0.1 μm. The width of the triangular traps varies along the template, as seen in Fig. 4 and fig. S2.

Particle assembly

The assembly was carried out using the setup and protocol described by Malaquin *et al.* (*18*). The assembly speed was kept between 1 and 2 μm s^{-1}. The assembly temperature was set at 10° to 15°C above the dew point. The assembly of the fourth particle on top of the open trimers was conducted with a higher surfactant concentration and lower surface tension (0.25 mM SDS and 0.025 wt % Triton X-45). The corresponding shallower angle of the moving droplet favors the trapping of the fourth particle because of the stronger confinement in the front part of the meniscus (*25*).

Printing, linking, and harvesting

The assembled particles can be printed onto silicon substrates with a thin adhesion layer using microcontact printing (*26*). For harvesting, the clusters assembled on the template were linked by a heating step at 75°C for 10 min. Extended heating for longer times or at higher temperatures may lead to significant deformation of the polymer particles. Harvesting of clusters was carried out by freezing (see Fig. 6): A 20-μl Millipore water droplet was placed on the area of interest of the template and then frozen. The frozen drop was collected from the surface using a pipette tip and transferred to an Eppendorf tube. The harvesting was performed at different freezing temperatures: −20°, −80°, and −196°C. A lower temperature enables longer operation times when picking up the frozen drop before it melts. However, at lower temperatures, clusters composed of different materials can crack in the neck between the particles because of the different thermal expansion coefficients (see fig. S7).

Imaging

Assembled, printed, harvested, and dried particle clusters were imaged by bright-field, dark-field, and fluorescence optical microscopy (Zeiss Axioscope) at various magnifications and by SEM (Leo 1550 Gemini, Carl Zeiss AG). ImageJ (W. S. Rasband, National Institutes of Health, Bethesda, MD) was used to compose merged fluorescence images and overlays of fluorescence and bright-field images by combining different channels. EDX characterization was performed using X-max (Oxford Instruments) in a scanning electron microscope (SU8000, Hitachi). The images in Fig. 7D and the corresponding supplementary movies were acquired in Millipore water on an inverted optical microscope (Zeiss Axioscope 2) with a 63× long working distance air objective. Images were grabbed at a frame rate of 10 fps using an Andor Zyla camera mixing the transmission and fluorescence channels. All other supplementary movies were acquired at varying frame rates, as specified in the Supplementary Materials.

Manipulation of clusters in a magnetic field

The colloidal surfactant chains with a magnetic head were harvested and dispersed in Millipore water. They were rotated and oscillated using an external magnetic field (1 Hz for rotation; 0.5 Hz and 270° rotation amplitude for oscillation). The magnetic fields are applied by two pairs of electromagnets driven by two independent current amplifiers controlled by custom LabVIEW software. The translation of the particles was performed by placing a permanent magnet close to the sample.

SUPPLEMENTARY MATERIALS

Supplementary material for this article is available at http://advances.sciencemag.org/cgi/content/full/2/4/e1501779/DC1

Technical details of the assembly of linear colloidal chains.

Technical details of the assembly of nonlinear colloidal clusters (trimers and 3D clusters).

Fig. S1. SEM images of different colloidal chains on the template.

Fig. S2. Effect of trap size on the assembly yield of R-G-B PS trimers.

Fig. S3. Yield of assembled carboxylate PS and amine PS dumbbells on an area of 5 × 12 mm^2.

Fig. S4. EDX spectroscopy of three-particle chains with plain SiO_2, PS, and magnetic SiO_2.

Fig. S5. Linking of clusters by thermal sintering.

Fig. S6. Harvesting of clusters.

Fig. S7. Harvesting of clusters at extremely low temperatures.

Fig. S8. Effects of varying lateral trap dimensions on the structure of 3D clusters.

Fig. S9. Effects of local assembly direction on the first sCAPA step of colloidal trimers.

Fig. S10. Effects of local assembly direction on the assembly of open colloidal trimers with three different lobes.

Movie S1. The first assembly step for the fabrication of surfactant-like colloidal chains.

Movie S2. The second assembly step for the fabrication of surfactant-like colloidal chains.

Movie S3. Brownian motion of a dumbbell with a magnetic head and a PS lobe dispersed in water after harvesting.
Movie S4. Brownian motion of a four-particle chain with a magnetic head and a PS tail dispersed in water after harvesting.
Movie S5. Brownian motion of an eight-particle chain with a magnetic head and a PS tail dispersed in water after harvesting.
Movie S6. Rotation of colloidal chains with a magnetic head in an external rotating magnetic field.
Movie S7. Oscillation of colloidal chains with a magnetic head in an external oscillating magnetic field.
Movie S8. Translation of a colloidal chain with a magnetic head by a permanent magnet.
Movie S9. The third assembly step for the fabrication of open PS trimers with three different lobes.

REFERENCES AND NOTES

1. W. Poon, Colloids as big atoms. *Science* **304**, 830–831 (2004).
2. E. V. Shevchenko, D. V. Talapin, N. A. Kotov, S. O'Brien, C. B. Murray, Structural diversity in binary nanoparticle superlattices. *Nature* **439**, 55–59 (2006).
3. F. Li, D. P. Josephson, A. Stein, Colloidal assembly: The road from particles to colloidal molecules and crystals. *Angew. Chem. Int. Ed. Engl.* **50**, 360–388 (2011).
4. N. Vogel, M. Retsch, C.-A. Fustin, A. del Campo, U. Jonas, Advances in colloidal assembly: The design of structure and hierarchy in two and three dimensions. *Chem. Rev.* **115**, 6265–6311 (2015).
5. L. Cademartiri, K. J. M. Bishop, Programmable self-assembly. *Nat. Mater.* **14**, 2–9 (2015).
6. M. R. Jones, C. A. Mirkin, Materials science: Self-assembly gets new direction. *Nature* **491**, 42–43 (2012).
7. S. C. Glotzer, M. J. Solomon, Anisotropy of building blocks and their assembly into complex structures. *Nat. Mater.* **6**, 557–562 (2007).
8. G.-R. Yi, D. J. Pine, S. Sacanna, Recent progress on patchy colloids and their self-assembly. *J. Phys. Condens. Matter* **25**, 193101 (2013).
9. J. Zhang, E. Luijten, S. Granick, Toward design rules of directional Janus colloidal assembly. *Annu. Rev. Phys. Chem.* **66**, 581–600 (2015).
10. Y. Wang, Y. Wang, D. R. Breed, V. N. Manoharan, L. Feng, A. D. Hollingsworth, M. Weck, D. J. Pine, Colloids with valence and specific directional bonding. *Nature* **491**, 51–55 (2012).
11. A. Perro, E. Duguet, O. Lambert, J.-C. Taveau, E. Bourgeat-Lami, S. Ravaine, A chemical synthetic route towards "colloidal molecules". *Angew. Chem. Int. Ed. Engl.* **48**, 361–365 (2009).
12. A. A. Shah, B. Schultz, W. Zhang, S. C. Glotzer, M. J. Solomon, Actuation of shape-memory colloidal fibres of Janus ellipsoids. *Nat. Mater.* **14**, 117–124 (2015).
13. Q. Chen, S. C. Bae, S. Granick, Directed self-assembly of a colloidal kagome lattice. *Nature* **469**, 381–384 (2011).
14. A. Perro, S. Reculusa, S. Ravaine, E. Bourgeat-Lami, E. Duguet, Design and synthesis of Janus micro- and nanoparticles. *J. Mater. Chem.* **15**, 3745–3760 (2005).
15. A. B. Pawar, I. Kretzschmar, Fabrication, assembly, and application of patchy particles. *Macromol. Rapid Commun.* **31**, 150–168 (2010).
16. Y. Yin, Y. Lu, B. Gates, Y. Xia, Template-assisted self-assembly: A practical route to complex aggregates of monodispersed colloids with well-defined sizes, shapes, and structures. *J. Am. Chem. Soc.* **123**, 8718–8729 (2001).
17. T. Kraus, L. Malaquin, H. Schmid, W. Riess, N. D. Spencer, H. Wolf, Nanoparticle printing with single-particle resolution. *Nat. Nanotechnol.* **2**, 570–576 (2007).
18. L. Malaquin, T. Kraus, H. Schmid, E. Delamarche, H. Wolf, Controlled particle placement through convective and capillary assembly. *Langmuir* **23**, 11513–11521 (2007).
19. M. Collet, S. Salomon, N. Y. Klein, F. Seichepine, C. Vieu, L. Nicu, G. Larrieu, Large-scale assembly of single nanowires through capillary-assisted dielectrophoresis. *Adv. Mater.* **27**, 1268–1273 (2015).
20. A. Rey, G. Billardon, E. Lörtscher, K. Moth-Poulsen, N. Stuhr-Hansen, H. Wolf, T. Bjørnholm, A. Stemmer, H. Riel, Deterministic assembly of linear gold nanorod chains as a platform for nanoscale applications. *Nanoscale* **5**, 8680–8688 (2013).
21. V. Liberman, V. Liberman, C. Yilmaz, T. M. Bloomstein, S. Somu, Y. Echegoyen, A. Busnaina, S. G. Cann, K. E. Krohn, M. F. Marchant, M. Rothschild, A nanoparticle convective directed assembly process for the fabrication of periodic surface enhanced Raman spectroscopy substrates. *Adv. Mater.* **22**, 4298–4302 (2010).
22. J. A. Fan, K. Bao, L. Sun, J. Bao, V. N. Manoharan, P. Nordlander, F. Capasso, Plasmonic mode engineering with templated self-assembled nanoclusters. *Nano Lett.* **12**, 5318–5324 (2012).
23. N. J. Greybush, M. Saboktakin, X. Ye, C. D. Giovampaola, S. J. Oh, N. E. Berry, N. Engheta, C. B. Murray, C. R. Kagan, Plasmon-enhanced upconversion luminescence in single nanophosphor–nanorod heterodimers formed through template-assisted self-assembly. *ACS Nano* **8**, 9482–9491 (2014).
24. X. Zhou, Y. Zhou, J. C. Ku, C. Zhang, C. A. Mirkin, Capillary force-driven, large-area alignment of multi-segmented nanowires. *ACS Nano* **8**, 1511–1516 (2014).
25. S. Ni, J. Leemann, H. Wolf, L. Isa, Insights into mechanisms of capillary assembly. *Faraday Discuss.* **181**, 225–242 (2015).
26. S. Ni, M. J. K. Klein, N. D. Spencer, H. Wolf, Cascaded assembly of complex multiparticle patterns. *Langmuir* **30**, 90–95 (2014).
27. M. J. K. Klein, C. Kuemin, T. Tamulevicius, M. Manning, H. Wolf, Note: A microfluidic chip setup for capillarity-assisted particle assembly. *Rev. Sci. Instrum.* **83**, 086109 (2012).
28. J. Yan, S. C. Bae, S. Granick, Colloidal superstructures programmed into magnetic Janus particles. *Adv. Mater.* **27**, 874–879 (2015).
29. A. Ghosh, P. Fischer, Controlled propulsion of artificial magnetic nanostructured propellers. *Nano Lett.* **9**, 2243–2245 (2009).
30. S. Tottori, S. Tottori, L. Zhang, F. Qiu, K. K. Krawczyk, A. Franco-Obregón, B. J. Nelson, Magnetic helical micromachines: Fabrication, controlled swimming, and cargo transport. *Adv. Mater.* **24**, 811–816 (2012).
31. T. D. Edwards, Y. Yang, D. J. Beltran-Villegas, M. A. Bevan, Colloidal crystal grain boundary formation and motion. *Sci. Rep.* **4**, 6132 (2014).
32. D. Zerrouki, J. Baudry, D. Pine, P. Chaikin, J. Bibette, Chiral colloidal clusters. *Nature* **455**, 380–382 (2008).
33. D. Nagao, M. Sugimoto, A. Okada, H. Ishii, M. Konno, A. Imhof, A. van Blaaderen, Directed orientation of asymmetric composite dumbbells by electric field induced assembly. *Langmuir* **28**, 6546–6550 (2012).
34. J. Lee, P. W. Bisso, R. L. Srinivas, J. J. Kim, A. J. Swiston, P. S. Doyle, Universal process-inert encoding architecture for polymer microparticles. *Nat. Mater.* **13**, 524–529 (2014).
35. Y. Zhao, Y. Cheng, L. Shang, J. Wang, Z. Xie, Z. Gu, Microfluidic synthesis of barcode particles for multiplex assays. *Small* **11**, 151–174 (2015).
36. L. Isa, N. Samudrala, E. R. Dufresne, Adsorption of sub-micron amphiphilic dumbbells to fluid interfaces. *Langmuir* **30**, 5057–5063 (2014).
37. A. Kumar, B. J. Park, F. Tu, D. Lee, Amphiphilic Janus particles at fluid interfaces. *Soft Matter* **9**, 6604–6617 (2013).
38. K. V. Edmond, M. T. Elsesser, G. L. Hunter, D. J. Pine, E. R. Weeks, Decoupling of rotational and translational diffusion in supercooled colloidal fluids. *Proc. Natl. Acad. Sci. U.S.A.* **109**, 17891–17896 (2012).
39. J. D. Forster, J.-G. Park, M. Mittal, H. Noh, C. F. Schreck, C. S. O'Hern, H. Cao, E. M. Furst, E. R. Dufresne, Assembly of optical-scale dumbbells into dense photonic crystals. *ACS Nano* **5**, 6695–6700 (2011).
40. A.-P. Hynninen, J. H. J. Thijssen, E. C. M. Vermolen, M. Dijkstra, A. van Blaaderen, Self-assembly route for photonic crystals with a bandgap in the visible region. *Nat. Mater.* **6**, 202–205 (2007).
41. B. H. McNaughton, K. A. Kehbein, J. N. Anker, R. Kopelman, Sudden breakdown in linear response of a rotationally driven magnetic microparticle and application to physical and chemical microsensing. *J. Phys. Chem. B* **110**, 18958–18964 (2006).
42. J. Li, W. Gao, R. Dong, A. Pei, S. Sattayasamitsathit, J. Wang, Nanomotor lithography. *Nat. Commun.* **5**, 5026 (2014).
43. M. Geissler, H. Wolf, R. Stutz, E. Delamarche, U.-W. Grummt, B. Michel, A. Bietsch, Fabrication of metal nanowires using microcontact printing. *Langmuir* **19**, 6301–6311 (2003).

Acknowledgments: We thank E. Marini for supplying the sample for fig. S6A, U. Drechsler and S. Reidt for help with the mask and master fabrication, A. Knoll and U. Duerig for discussions and advice, C. Bolliger for assistance with the manuscript, and R. Allenspach and W. Riess for continuous support. **Funding:** L.I., S.N., and I.B. acknowledge financial support from the Swiss National Science Foundation (grant PP00P2_144646/1). **Author contributions:** S.N., L.I., and H.W. conceived and designed the study. S.N. and J.L. performed the sCAPA assembly and characterized the results. S.N. and H.W. developed the harvesting protocol. S.N., I.B., and L.I. performed the optical microscopy and magnetic manipulation experiments. All authors analyzed the data. S.N., L.I., and H.W. wrote the manuscript. All authors discussed the results and commented on the manuscript. **Competing interests:** The authors declare that they have no competing interests. **Data and materials availability:** All data needed to evaluate the conclusions in the paper are present in the paper and/or the Supplementary Materials. Additional data related to this paper may be requested from the authors.

Submitted 7 December 2015
Accepted 13 February 2016
Published 1 April 2016
10.1126/sciadv.1501779

Citation: S. Ni, J. Leemann, I. Buttinoni, L. Isa, H. Wolf, Programmable colloidal molecules from sequential capillarity-assisted particle assembly. *Sci. Adv.* **2**, e1501779 (2016).